EEG Signals Classification related to Visual Objects using Long Short-Term Memory Network and Nonlinear Interval Type-2 Fuzzy Regression

Hajar Ahmadieh
Amirkabir university
Farnaz Gassemi (Ghassemi@aut.ac.ir)
Amirkabir university
Mohammad Hasan Moradi
Amirkabir university

Research Article

Keywords: LSTM network, ResNet network, visual image classification, EEG signal, nonlinear fuzzy regression

Posted Date: September 15th, 2023

DOI: https://doi.org/10.21203/rs.3.rs-3317817/v1

Additional Declarations: No competing interests reported.

EEG Signals Classification related to Visual Objects using Long Short-Term Memory Network and Nonlinear Interval Type-2 Fuzzy Regression

Hajar Ahmadieh[1]. Farnaz Gassemi[2]. Mohammad hasan Moradi[3]

Abstract

By comprehending how brain activity is encoded and decoded, we can better comprehend how the brain functions. This study presents a method for classifying EEG signals from visual objects that combines an LSTM network with nonlinear interval type-2 fuzzy regression (NIT2FR). Here, ResNet is used to extract features from the images, the LSTM network is used to extract features from the EEG signal, and NIT2FR is used to map the features from the images to the features from the EEG signal. In this paper, type-2 fuzzy logic is utilized to handle this type of uncertainty due to the nonlinearity and noise of the EEG signals, the short sample size of the data, and the varied mental backgrounds of the experiment participants. The Stanford database was used to implement the research technique, and its effectiveness was assessed using the classification accuracy, precision, recall, and F1 score. The LSTM network successfully categorized images using raw EEG data with an accuracy of 55.83%, according to the findings. When compared to classification accuracy obtained with linear type-2, linear and nonlinear type-1 fuzzy, neural network, and polynomial regression, NIT2FR and SVM classifier performed better (68.05%). NIT2FR can therefore perform better in settings with high levels of uncertainty. Additionally, the accuracy outcomes using NIT2FR are 6.03% better than the top outcome of the most recent study that made use of the same dataset. The same process was followed to get the same result for the other performance raters.

Keywords: LSTM network, ResNet network, visual image classification, EEG signal, nonlinear fuzzy regression.

1. Introduction

One of the most important concerns in neuroscience is neural coding, which describes the relationship between stimulus and response of a single neuron or the neuronal group and the electrical activity of nerves in this group (Brown, Kass, and Mitra 2004). Human brain data can be utilized to decode human thoughts and actions, as well as to diagnose mental diseases. Machine learning (ML) method is one of the important techniques in research fields, therefore, it has been widely used in fields other than artificial intelligence such as medicine to extract information from brain data (Janssen, Mourão-Miranda, and Schnack 2018). Deep learning methods are used in several EEG-based brain computer interface (BCI) devices. For example, consider a person with paralysis controlling mobility assistance (Münßinger et al. 2010; Nijboer et al. 2008; Tonin et al. 2011). These are also used to aid rehabilitation in stroke and treat epilepsy (Gadhoumi et al. 2016; Malmivuo, Ahokas, and Välkky 2014). The use of machine learning to decode fMRI and EEG data, as well as the number and quality of decoding, has increased dramatically in this area. Decoding the relationship between stimuli and neuronal responses has been used with applications such as classifying (Kamitani and Tong 2005) or recognizing and reconstructing the image seen by the participant (Miyawaki et al. 2008). EEG signal is one of the most important biological signals that encodes information about the human internal states. Because of its accessibility, low cost, and ease of use, EEG signals have garnered considerable attention. Given the high temporal resolution of electroencephalogram (EEG) signals and the unique patterns in the EEG signal when a person is watching images, detecting and classifying images with

✉ Farnaz Gassemi
ghassemi@aut.ac.ir

Hajar Ahmadieh
h.ahmadieh@ aut.ac.ir

Mohammad hasan Moradi
mhmoradi@aut.ac.ir

1,2,3 Department of Biomedical Engineering, Amirkabir University of Technology, Tehran, IRAN.

this signal appears to be a viable method (Malmivuo, Ahokas, and Välkky 2014; Yu et al. 2019). The number of research that have employed the EEG signal for this purpose, however, is quite small. We propose to introduce a new method in this article that employs the EEG signal class to identify the visuals shown to the individual.

In general, the classification of visual images with EEG consists of four phases. Preprocessing, feature extraction, feature selection, and classification are the four phases. Prior to 2017, shallow methods were used for this purpose. Wavelet (Taghizadeh-Sarabi, Daliri, and Niksirat 2015), event-related potentials (Daliri, Taghizadeh, and Niksirat 2013), amplitude-amplitude coupling (AAC), phase–phase coupling (PPC), phase–amplitude coupling (PAC) (Jafakesh, Jahromy, and Daliri 2016), and Functional connectivity measures (Tafreshi, Daliri, and Ghodousi 2019) were used as features extraction methods in these studies. Deep learning technologies were first used for this purpose by researchers in 2017. Spampinato et al., for example, used Long Short-Term Memory (LSTM) and Recurrent Neural Networks (RNN) to extract features from the EEG signal and Convolutional Neural Network (CNN) to extract features from images, followed by a CNN regression to map the extracted image features on the extracted signal features in (Spampinato et al. 2017). Based on the results, the classification accuracy for 40 classes was 82.9%. Following that, in (Fares, Zhong, and Jiang 2018), researcher employed bi-directional LSTM instead of simple LSTM in (Spampinato et al. 2017) and ICA for classification. In addition, in (Zheng et al. 2020), LSTM with Swich activity function was used instead of simple LSTM, ResNet instead of CNN and K-Nearest Neighbor (KNN) regression, Random Forest (RF) and Support Vector Regression (SVR) instead of CNN regression in (Spampinato et al. 2017). The classification accuracy in these two papers was 97.1% in (Fares, Zhong, and Jiang 2018) and 97.13% in (Zheng et al. 2020) for 40 classes. Using LSTM and Generative Adversarial Networks (GANs), The authors were able to classify the images seen by the participants with an average classification accuracy of 43% for 40 classes in (Palazzo et al. 2017; Tirupattur et al. 2018). Also, they reconstructed the images using the mentioned network.

In (Alazrai et al. 2022), the authors proposed a new method for decoding imagined numbers and letters in the minds of participants. This method is divided into two parts. The Choi-Williams time-frequency distribution (CWD) is used in the first part to represent the time, frequency and spatial (TFS) structure of EEG signal. In the second step, a deep network is used to extract features from the previously obtained distribution. In this way, the classification accuracy for numbers and letters was 95.47 ± 2.3%.

Another approach for classifying the visual image has been presented in (McCartney et al. 2019). The dataset used in this paper is Trento and Stanford (Kaneshiro et al. 2015; Murphy, Baroni, and Poesio 2009). To extract features from images, the Gabor filter, the Scale Invariant Feature Transform (SIFT), the color histogram -hue, saturation, and value- (HSV), and Global Vectors (GloVe) have been used. These four models were combined to form a structure that is similar to the structure of the brain's visual cortex under visual stimulation. The Pearson correlation coefficient was applied for extracting features from the EEG signals. The third step involved using linear regression to map features extracted from images onto features extracted from EEG signals. The Cumulative Match Curve (CMC) is used in this evaluation method to represent the percentage of cases in which the target image is the closest distance to the predicted properties in the feature space. Finally, the Area Under Curve (AUC) is provided. Another paper that recently used these two databases (Kaneshiro et al. 2015; Murphy, Baroni, and Poesio 2009) for the same purpose is (McCartney, Devereux, and Martinez-del-Rincon 2022). In this paper, Inception V3 network is used to extract features from images and a deep neural network with different layers is used to extract features from EEG signal. A learning metric is then used to map these two features together. The classification accuracy in different modes has been obtained between 53.8 and 56.95.

In this research, the method employed in (Ahmadieh et al. 2023) is utilized to extract the feature from the EEG data, and a type of CNN network called ResNet is used to extract the feature from the images. The novelty of this paper lies in the feature mapper, which makes use of Nonlinear Interval Type-2 Fuzzy Regression (NIT2FR). Classic Takagi-Sugeno fuzzy models typically use zero- or one-degree polynomials in their consequent part (Takagi and Sugeno 1985). Researchers in (Ahmadieh et al. 2023) have used this fuzzy model to map the features extracted from visual images on the features extracted on the EEG signal. Nonlinear systems, as we know, can better approximate the desired function in a nonlinear environment. Thus, nonlinear Takagi-Sugeno fuzzy models, which are generalized classical models, can be a good alternative to classical models and produce better results (Park, Kim, and Oh 2000). As a result, we used this method to classify visual images. This paper consists of four sections. Materials and Methods is presented in the following section. Section 3 report on the experimental results and discussion. Last section is conclusion.

2. Materials and Methods

2.1. Type-2 fuzzy logic system background

Professor Lotfi Asgarzadeh introduced the fuzzy set in 1965. These sets were the basis for an effective method for modeling uncertainty and ambiguity (Zadeh 1965). The membership degrees in fuzzy systems are crisp. Therefore, it has limited ability to express uncertainty. In 1975, Prof. Zadeh introduced type-2 fuzzy sets as the development of type-1 fuzzy sets (Zadeh 1975). Unlike type-1 fuzzy sets, which have crisp membership functions, type-2 fuzzy sets have fuzzy membership functions, which can reduce the noise effect (Coupland and John 2008; Hisdal 1981). Fig. 1 depicts the structure of a general T2FLS. The structure of type-2 fuzzy is similar to that of a type-1 fuzzy logic system, with the exception that in the antecedent part of this structure, there is also type reduction in addition to the presence of a defizzifier.

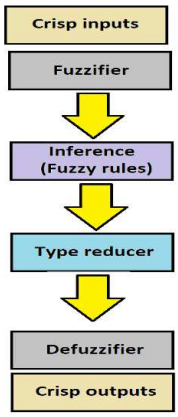

Fig.1 General structure of a T2FLS

2.1.1. Interval type-2 fuzzy logic system

Type-2 fuzzy systems are basically based on type-2 fuzzy sets. A general type-2 fuzzy set is depicted in Fig. 2. The interval type-2 fuzzy set is used for simplicity because the calculations for the general type-2 fuzzy set are so complex. Degrees of membership in an interval type-2 fuzzy set are expressed as interval for the third dimension's value. In other words, in interval type-2 fuzzy sets the third dimension is considered the same everywhere and is omitted. The only Footprint of Uncertainty (FOU) (The region bounded by upper membership function (UMF) and lower membership function (LMF) of the IT2FS is called FOU shown in Fig. 2) is used in interval type-2 fuzzy sets (Nguyen et al. 2015).

2.1.2. Takagi-Sugeno fuzzy logic systems

Takagi-Sugeno fuzzy system (Takagi and Sugeno 1985) was introduced in 1985 as a new fuzzy system. The Takagi-Sugeno fuzzy system's output is simple to compute, and its parameters can be modified using adaptive optimization techniques, particularly gradient descent algorithms. Takagi-Sugeno type-2 fuzzy system is an interval fuzzy structure that employs type-2 membership functions in the antecedent and the zero and one polynomial in the consequent. The learning operation, like adaptive networks in the Takagi-Sugeno system with orders zero and one, is a process that leads to the determination of the parameters of the input membership functions and the coefficients of the functions of the sequence of rules. In this case, the obtained fuzzy system can calculate the output value by receiving the new input values with the least difference from the estimated function values.

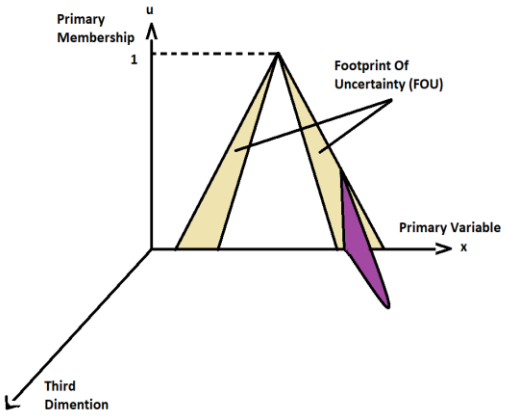

Fig. 2 Membership function of a general type-2 fuzzy set in three dimensions.

2.1.3. Nonlinear interval type-2 fuzzy regression (NIT2FR)

Regression expresses the relationship between independent and dependent variables statistically rather than mathematically. This means that the value of y for every x is not completely clear and precise, and determining its value is associated with an error value. The type of the relationship between independent and dependent variables varies. But in general, the statistical model is considered as $\hat{y}_i = f(x_i, B)$ where $y_i = \hat{y}_i + \epsilon_i$, x_i represents the independent variable, $\hat{y}_i$ is the estimated dependent variable, y_i is the actual value of a dependent variable, B is the parameters, and ϵ_i is the error. After determining the type of relationship, the first step is to estimate the model's unknown parameters, this completes the model and allows it to predict the values of y as a function of the new x. NIT2FR is used as a function in this paper to map the features extracted from the image to the features extracted from the EEG signal. As a result of combining these features with the unknown function, the NIT2FR can be trained to be an approximation of this function with the shortest distance to the feature values.

In this paper, we use an input variable with 100 dimensions that is the features extracted from the EEG signal. As previously stated, only the first part of the system, not the y_i part of the fuzzy system, has a linguistic interpretation. Fig. 3 depicts the structure of a type-2 fuzzy network, which is made up of five layers as follows:

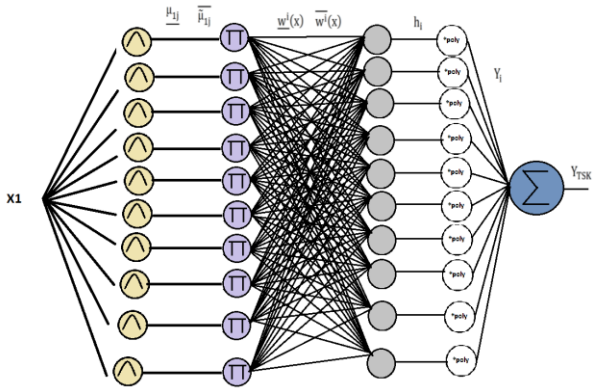

Fig. 3 The structure of the type-2 fuzzy network

Layer 1: Input variables pass through membership functions. Gaussian membership functions were chosen because they use only two parameters for learning (mean and variance), which reduces computation time and simplifies optimization (Wu 2012). Fig. 4 depicts the Gaussian membership function.

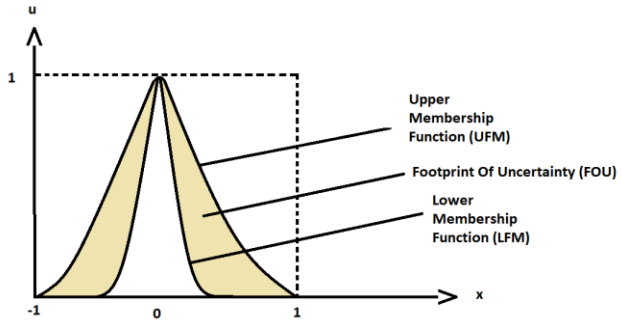

Fig. 4 A sample interval type-2 Gaussian with lower and upper fuzzy set

Layer 2: This layer defines fuzzy rules (firepower). Eq. 1 defines the ith fuzzy rule:

$$W^i = \left[\underline{w}^i(x), \overline{w}^i(x)\right] \qquad i = 1,2,\dots,r \tag{1}$$

Where $\underline{w}^i(x), \overline{w}^i(x)$ are defined as Eq. 2

$$\begin{aligned} \underline{w}^i &= \prod_{a=1}^{n} \underline{\tilde{\mu}}_a{}^i(x_a) \\ \overline{w}^i &= \prod_{a=1}^{n} \overline{\tilde{\mu}}_a{}^i(x_a) \end{aligned} \tag{2}$$

Where $\underline{\tilde{\mu}}_a{}^i$, $\overline{\tilde{\mu}}_a{}^i$ are lower and upper grades of membership that are calculated at layer 1 and n is the number of network inputs. Here because there is only one input, upper and lower membership are equivalent to the upper and lower firepower.

Layer 3: The normalized firepower of any rule is calculated in this layer by Eq. 3:

$$h_i = \frac{\overline{w}^i + \underline{w}^i}{\sum_{i=1}^{r} \underline{w}^i + \sum_{i=1}^{r} \overline{w}^i} \tag{3}$$

Layer 4: The normalized firepower is multiplied by the function of the consequent variables (here is a third-degree polynomial) in this layer as Eq. 4:

$$y_i = h_i * \sum_{d=0}^{3} \theta_d{}^i x^d \tag{4}$$

Where θ corresponds to the polynomial coefficients used in the consequent part.

Layer 5: The output of the NIT2FR is obtained with Eq. 5:

$$Y_{TSK} = \sum_{i=1}^{r} y_i \tag{5}$$

2.2. NIT2FR combined with LSTM and ResNet for EEG signal classification

The goal of this paper is to develop methods for classifying visual objects. The class of images that the participant is watching has been identified using EEG data evoked by visual object stimuli. Because RNN networks are useful for signal temporal analysis, this network was used to learn the features of the EEG signal. Of course, expecting this network to achieve high classification accuracy on its own is unrealistic. As a result, the next step is to use the ResNet network to extract the visual image features, which will then be transferred to EEG features. The image features are then mapped to the EEG signal features using nonlinear interval type-2 and type-1 fuzzy regressions to improve classification accuracy in the first step, which is only from the LSTM network. Finally, for classifying new features, a support vector machine (SVM) will be used. Fig. 5 depicts the steps described above.

It should be noted that the preceding steps are related to the training phase, and in the test phase, part 2 in Fig. 5 is removed, and the class related to each new EEG signal is detected using the trained LSTM network, regression, and classifier. According to our knowledge, this is the first time that nonlinear interval type-2 and type-1 fuzzy regression

have been used as image feature mappers to EEG features, and these regressions have been compared with linear type-1 and-2 fuzzy, neural network, and polynomial regression in this paper.

2.2.1. LSTM Network

Recurrent neural networks (RNN) are so-called memory because the output of each layer depends on the parameters of the previous layer This network is ideal for time series analysis due to its memory and ability to predict time series. These networks were created to overcome the limitations of feedforward networks. Although this network can store sequence information, it can only do so for a finite number of previous sequences. In other words, it has limited memory. Hochreiter and Schmidhuber (Hochreiter and Schmidhuber 1997)introduced LSTM (depicted in Fig. 6) to develop and solve this problem. The ability to learn long-term dependencies, which was not possible with recursive neural networks, is the most important feature of LSTM. Furthermore, the vanishing gradient problem, which is solved by LSTM networks with self-connected linear recurrent units called constant error carousel (CECs), is one of the problems with RNN networks (Gers 2001).

The activation calculation method in LSTM differs significantly from that in conventional RNN cells. In step t, activation is calculated using the cell state and three types of gates: input gate, forget gate, and output gate (Fang and Yuan 2019).

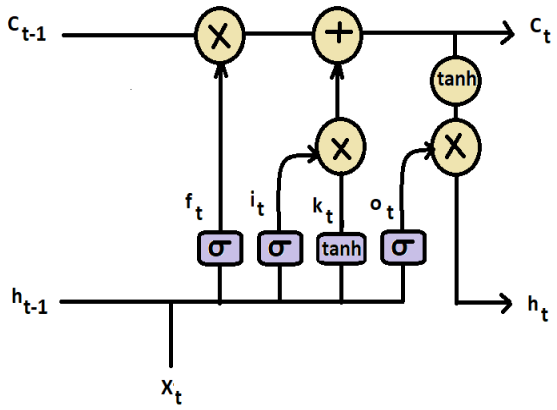

Fig. 6 The long short-term memory (LSTM) unit contains an input gate, a forget gate, and an output gate. σ represents the sigmoid activation function while tanh represents a tangent hyperbolic activation.

In step t, the values of the input, forget, and output gates are calculated using Eq.s 6, 7, and 8 respectively:

$$i_t = \sigma(W_{ia}.h_{t-1} + W_{ix}.x_t) \quad (6)$$
$$f_t = \sigma\left(W_{fa}.h_{t-1} + W_{fx}.x_t\right) \quad (7)$$
$$o_t = \sigma(W_{oa}.h_{t-1} + W_{ox}.x_t) \quad (8)$$

Where σ is a nonlinear function like the sigmoid function. W_{ia} , W_{fa}, and W_{oa} are weight matrices that connect h_{t-1} to h_t and W_{ix} , W_{fx} , and W_{ox} are weight matrices that connect x_t to h_t, respectively in input, forget, and the output gate.

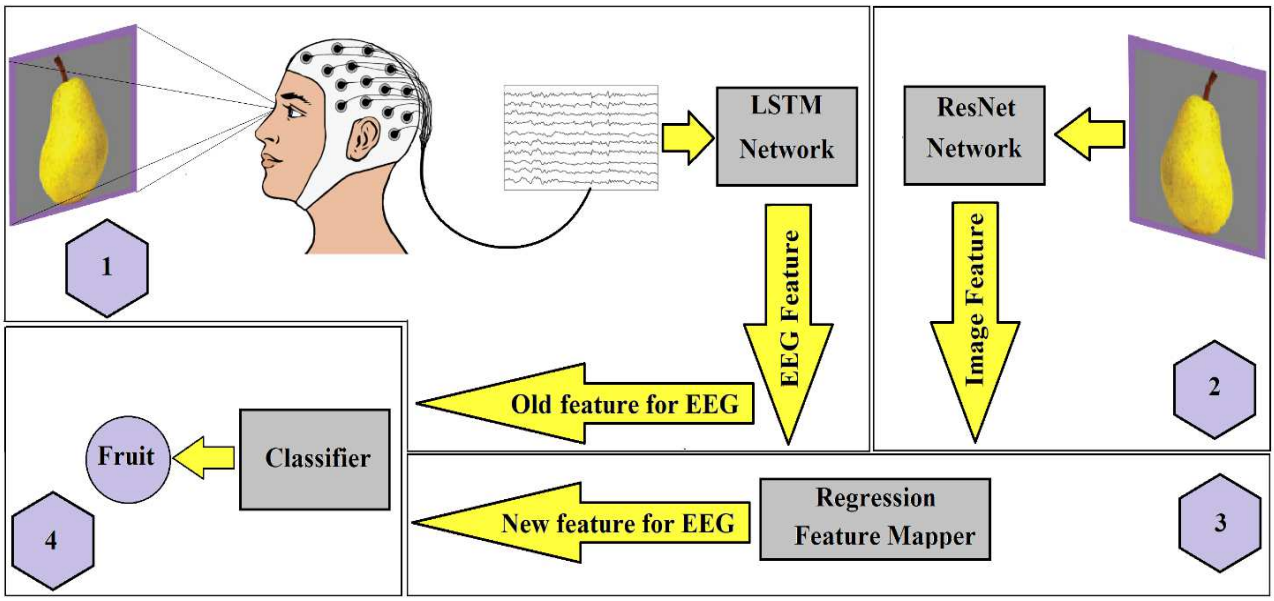

Fig. 5 Visual image classification process. Brain activity is recorded by the EEG signal when seeing an image, and the visual image is then classified from brain data using a computational model.

The input of the cell is calculated as Eq. 9:

$$C_t = f_t . C_{t-1} + i_t . k_t \quad (9)$$

Where C_{t-1} is cell state information from the previous step and k_t is calculated as Eq. 10:

$$k_t = \tanh (W_{ca} . h_{t-1} + W_{cx} . x_t) \quad (10)$$

Finally, h_t is calculated as Eq. 11:

$$h_t = o_t . tanh(C_t) \quad (11)$$

Because of its ability in time series analysis, this network is used in this paper to extract the EEG time series feature.

The LSTM network, like any other network, has its own parameters that must be set before training. These parameters include the recurrent depth, batch size, number of training periods, LSTM hidden layer size, dropout rates applied after the input layer, and the LSTM layer's L2 matrix weight adjustment factor. Adam's approach is used for network optimization in this article (Kingma and Ba 2014).

2.2.2. ResNet

The convolutional network is inspired by the visual cortex of the brain. The layers of this network are so similar to the cerebral cortex that a one-to-one relationship can be found between the activity of neurons in the cortical layers and the layers of convolutional networks such as AlexNet convolutional neural networks (Krizhevsky, Sutskever, and Hinton 2012). This similarity in neuronal activity exists when the convolutional network is not optimized to predict brain activity and is trained to detect objects and images. Following research has revealed that this similarity exists even in more complex networks like ResNet (He et al. 2016; Wen et al. 2018). According to numerous studies, as network depth increases, so does network accuracy (Piccialli et al. 2021). However, as the depth of the network increases, everything changes and the error begins to increase; this is known as "Degradation".

To address this issue, the Microsoft group introduced the very deep Resent network with 152 layers in 2016 (He et al. 2016). Instead of the main layer, blocks known as residuals have been used in this network. This residual block is made up of the sum of two residual mapping functions as well as the identity function (see Fig. 7). Given a learning map $H(x)$, the first layer of a residual block learns from the residual function F(x)=H(x)-x. While the second layer learns from the function $G(x) = x$. By using this block in the Resent network, researchers were able to solve the problems related to the reduction of accuracy in relation to the classification of images. (Piccialli et al. 2021; Wang et al. 2017). Finally, by placing several residual blocks in a row to reduce the error, a very deep network can be designed that does not face the problem of degradation with increasing depth. Fig. 8 shows the deep structure of the ResNet network. This Fig. shows a 50-layer model of this network. In this paper, we have used this 50-layer convolutional network that had been pre-trained on ImageNet images to extract image features.

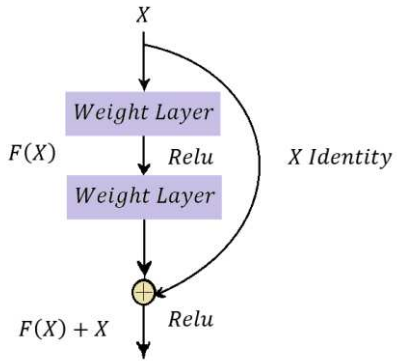

Fig. 7 An example of a residual block in the ResNet network.

The deeper the network, the better the learning, but the calculations become more complicated and more training data is needed to train that network. Transfer learning involves training a very deep network on a large database, and then adapting this trained network to insufficient data for the desired application (Acharya et al. 2018; Byra et al. 2018; Craik, He, and Contreras-Vidal 2019; Khan et al. 2019; Shin et al. 2016). In other words, we transfer the trained network with trained parameters on a large database to an insufficient database for our application. This approach has advantages such as shorter learning time, lower computational load, less data and therefore weaker hardware. In this method, images that were resized are presented as input to the network. Convolutional layer and poling layer of the Resent network are as feature extractor and fully connected layer and softmax layer as classification layer.

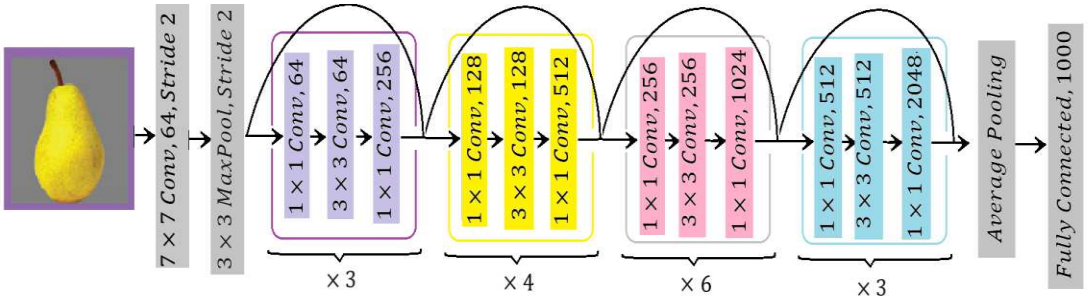

Fig. 8 Example of ResNet network with 50-layer

2.2.3 Training NIT2FLS using gradient descent algorithm

In this section, an error function was defined for mapping the features extracted from the images by ResNet to the features extracted from the EEG signal by LSTM in Eq. 12 and tried to minimize this error:

$$E = \frac{1}{2}(Yimage - Y_{TSK})^2 \tag{12}$$

Where $Yimage$ represents features extracted from the images and Y_{TSK} represents the features extracted from the EEG signal after passing through the NIT2FR.

As previously stated, θ_d^i in Eq. 4 is the consequent parameter. w^i has two adjustable parameters including mean and variance (with Gaussian membership function), which are called antecedent parameters. The gradient descent algorithm is used to obtain the parameters, including the antecedent and consequent. The antecedent parameters are then updated using Eq. 13:

$$\begin{aligned}\theta(t+1) &= \theta(t) - \gamma\frac{\partial E}{\partial \theta} \\ &= \theta(t) - \gamma\frac{\partial E}{\partial Y_{TSK}} * \frac{\partial Y_{TSK}}{\partial \overline{w}^i} * \frac{\partial \overline{w}^i}{\partial \theta} \\ &+ \gamma\frac{\partial E}{\partial Y_{TSK}} * \frac{\partial Y_{TSK}}{\partial \underline{w}^i} * \frac{\partial \underline{w}^i}{\partial \theta}\end{aligned} \tag{13}$$

Where θ includes the mean and variance of fuzzy rules that are updated at each stage. Eq. 14 is then used to update the consequent parameters:

$$\begin{aligned}\theta(t+1) &= \theta(t) - \gamma\frac{\partial E}{\partial \theta} \\ &= \theta(t) - \gamma\frac{\partial E}{\partial Y_{TSK}} * \frac{\partial Y_{TSK}}{\partial \theta}\end{aligned} \tag{14}$$

Where θ is consequent parameter and γ is the learning rate which is chosen empirically and is updated at each step.

According to Eq.s 5 and 12, Eq.s 13 and 14 can be calculated.

3. Experimental Results

The obtained EEG signals are usually contaminated with noise due to the different mental backgrounds of people, involuntary motor activities such as blinking, etc.(Kappel et al. 2017). Because the type-2 fuzzy system performs better in environments with more noise and higher uncertainty, in this paper, the type-2 fuzzy logic system method is used and compared with type-1. Fig. 5 depicts all of the steps involved in the classification of visual objects, as previously explained. These steps are implemented in MATLAB2021a software.

3.1. Dataset

The dataset used in this paper was collected by Stanford University (Kaneshiro et al. 2015) and used in (McCartney et al. 2019) to classify visual images. Six groups of images including the human body, animal body, human face, animal face, fruits/vegetables and tools (12 images in each group) were randomly shown to the participants. This was done in 2 sessions consisting of 3 blocks, which showed a total of 5184 images to each participant. There were 10 participants, all of whom completed these two sessions and three separate EEG recordings per session so a total of 51840 images were shown to the participants. In each of these iterations, an EEG signal with 128 channels and 32 samples is recorded. The sampling frequency is 62.5 Hz. That is, each image is shown to the participant for about 0.5 seconds. Data preprocessing is done offline using MATLAB software. See (Kaneshiro et al. 2015) for more details on preprocessing and tasks.

3.2. Feature Extraction with LSTM, ResNet and NIT2FLS

According to Fig. 5 Part 1, Out of a total of 5,184 signals per participant (including 72 images shown to participants 72 times), one repetition of the signal obtained corresponding to each image is considered as test data and the rest as training data. So, in total there are 72 test signals for each person and 5112 training signals. Each of these samples has 128 (the number of electrodes) by 32 (the

number of time samples) signals. Out of 128 channels, 5 occipital channels according to Fig. 9 have been selected as LSTM network inputs (Visual Cortex). Therefore, LSTM network input is considered 5 by 32 in two dimensions. The number of features extracted from each EEG signal is considered to be 100. In this network, Adam, Sgdm, and Rmsprop's optimization algorithms are used and the Initial Learning Rate is equal to 0.001, L2 Regularization is equal to 0.005, and the loss model is cross entropy.

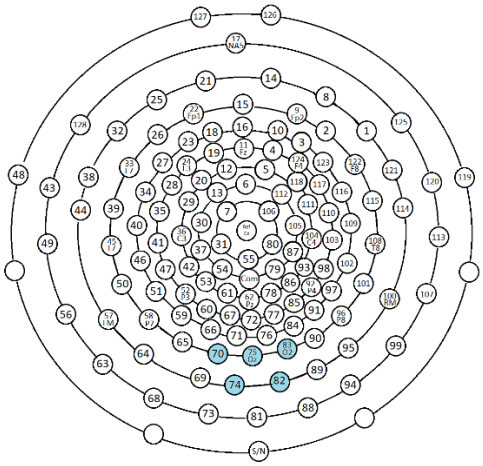

Fig. 9 Electrode arrangement for EEG recording with 128-channel EGI HCGSN 110 nets. The blue electrodes are the electrodes used to extract features from the EEG signal.

According to Fig. 5 part 2, because of the similarity of the ResNet network to the cerebral cortex, this network (pre-trained) is used to extract the features of the images. Fig. 10 depicts the 72 images shown to the participants. The number of features used in this section is 1000, which decreases to 100 after down-sampling.

In this step, nonlinear interval type-2 and type-1 fuzzy regressions are trained by the gradient descent algorithm to map the features extracted from the image on the features extracted from the EEG signal. In the test stage, with a trained NIT2FR and new EEG signal data, we can obtain EEG signal features that also contain image information. Neural network regression and polynomial regression were used to compare the performance of nonlinear and linear fuzzy regression. Neural network regression was optimized using the Adam algorithm and three-order polynomial regression was optimized using the gradient descent algorithm.

3.3. Classification Result

To evaluate the classification results, accuracy, precision, recall(sensitivity), and F1 score are used those relationships are defined as Eqs. 15-18.

$$Accuracy = \frac{TP + TN}{TP + FP + TN + FN} \tag{15}$$

$$Recall = \frac{TP}{TP + FN} \tag{16}$$

$$Precision = \frac{TP}{TP + FP} \tag{17}$$

$$F1Score = 2\frac{Precision * Recall}{Precision + Recall} = \frac{2TP}{2TP + FN + FP} \tag{18}$$

Where TP, TN, FP, and FN are True Positive, True Negative, False Positive, and False Negative respectively.

The most intuitive and main criterion used in this paper for evaluation is accuracy, which is defined as Eq. 15 but for further investigation precision and recall are used. precision is a measure of how many of the positive predictions made are correct and Recall is a measure of how many of the positive cases the classifier correctly predicted, over all the positive cases in the data (See Eqs. 16, 17). Another evaluation criterion is the F1 score, which is defined as the harmonic mean between the two criteria of precision and recall.

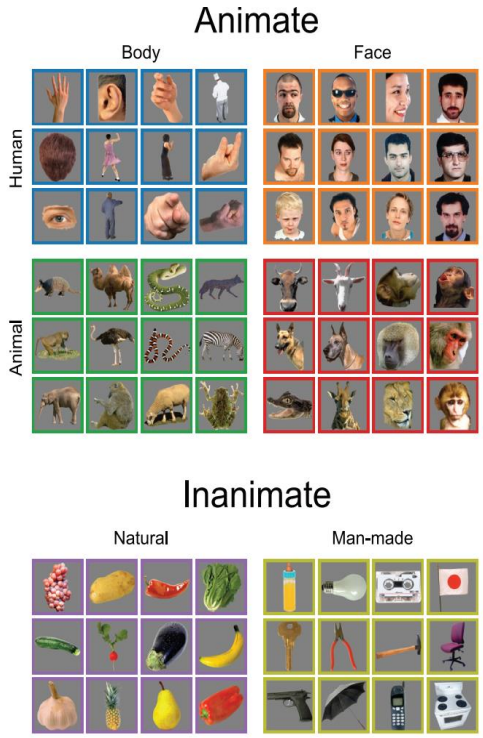

Fig. 10 Six groups of images (each group contains 12 images) were shown to the participants. (Kaneshiro et al. 2015).

Fig. 11 and Table 1 show the comparison of all the seven algorithms' performance in terms of accuracy, precision, recall, and F1 score for all participants (subject independent). As can be seen, the classification accuracy results of the proposed method of this article (the last two columns of Table 1) are better than the other 5 methods (the results obtained in the article (Ahmadieh et al. 2023)). This shows that by changing the activity function in the consequent part of the fuzzy network, this network was able to give better results in the environment with high uncertainty.

As we described before this in the LSTM network, Adam, Sgdm, and Rmsprop methods are used for optimization. Fig. 12 shows a comparison between these three optimizers. As can be seen, Adam's optimizer with the same conditions has higher accuracy than other optimizers in the case where all participants are present. Therefore, Adam's optimizer was used in continuing.

The results of the classification accuracy when the LSTM network is feature extractor and Softmax is classification are shown in Table 2, Row 1 for different participants (subject-dependent), all participants (subject-independent), and the average of all participants (Ahmadieh et al. 2023).

The features extracted from the LSTM output and the features extracted from ResNet for each image are then given to a nonlinear interval type-2 and -1 fuzzy regressions as input. Classification accuracy for each participant, all participants, and the mean of all participants with SVM classification is shown in Table 2 (rows 2, 3, 4, 5, 6, and 7). The classification accuracy in nonlinear interval type-2 and type-1 fuzzy regression is higher than the other regressions. Because the EEG signal has noise including ambient noise and blinking noise, etc. type-2 fuzzy performs better in environments with higher uncertainty and also has a higher degree of freedom than type-1, so NIT2FR outperforms nonlinear type-1 fuzzy regression. For linear type -1 and -2 fuzzy regression, the same results have been obtained too (Ahmadieh et al. 2023).

Table 3 shows the other three classifier evaluations (accuracy, recall and F1 score). As you can see, nonlinear fuzzy type 2 regression, which had higher accuracy, had higher precision and recall in different classes on average, and as a result, the F1 score was higher. Also, these evaluators show a higher value in two nonlinear type 1 and type 2 fuzzy algorithms than type 1 and 2 fuzzy on average. As you see in Fig. 13 nonlinear fuzzy regression in two modes (fuzzy 1 and 2) has better performance than linear fuzzy regression in both modes.

As described in Section 3.1, this paper uses the data set used in (Kaneshiro et al. 2015). According to our knowledge, only three articles (Ahmadieh et al. 2023; McCartney, Devereux, and Martinez-del-Rincon 2022; McCartney et al. 2019) have used this database to classify visual images. In (McCartney et al. 2019), classification accuracy for each participant separately, when all participants are considered together and the average classification accuracy for all participants for the three feature extraction approaches (including visual features, semantic features, and a combination of visual and semantic) has been reported. The mean classification accuracy for all individuals and for the three approaches are 58.08, 60.88, and 62.02, as reported in Table 4 (the last three columns of the last row) and Fig. 14. Likewise, the classification accuracy for the situation in which all participants are considered together and for the three approaches are 61.97, 64.82 and, 66.01, as reported in Table 4 (last three columns and first row) and Fig. 14. In (McCartney, Devereux, and Martinez-del-Rincon 2022) the classification accuracy in cases where the number of layers in the neural network used was changed was between 53.8 and 56.95.

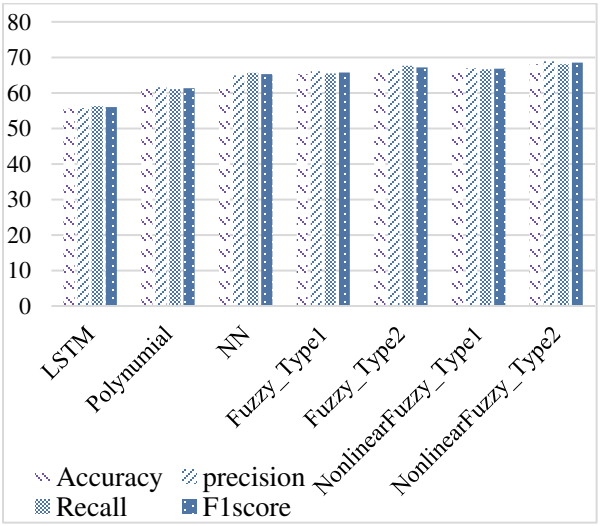

Fig. 11 performance of results of seven algorithms

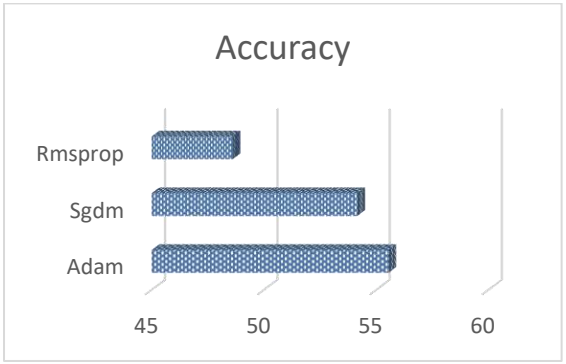

Fig. 12 Accuracy of classification with LSTM network and Softmax with different optimizers

Table 1 performance of results of seven algorithms

Feature Extraction from EEG: **Feature Extraction from Image:** **Feature Mapper:** **Classification:**	LSTM - - Softmax	LSTM ResNet Polynomial SVM	LSTM ResNet NN SVM	LSTM ResNet Fuzzy_Type1 SVM	LSTM ResNet Fuzzy_Type2 SVM	LSTM ResNet NIT1FR SVM	LSTM ResNet NIT2FR SVM
Accuracy	55.55	61.11	61.11	65.28	66.67	66.67	68.06
precision	55.73	61.62	64.93	66.07	66.66	66.89	68.93
Recall	56.30	61.05	65.61	65.45	67.64	66.66	68.05
F1score	56.01	61.33	65.27	65.76	67.15	66.77	68.49

Table 2 Classification accuracy in the different participants (subject-dependent), all participants (subject-independent) and mean of all participants

Method	**S1**	**S2**	**S3**	**S4**	**S5**	**S6**	**S7**	**S8**	**S9**	**S10**	**Mean**	**All participants**
LSTM (Number feature100) Classification=softmax (Ahmadieh et al. 2023)	56.94	55.55	58.33	48.61	56.94	59.72	54.16	54.16	58.33	55.55	**55.83**	**55.55**
LSTM+ResNet+ Polynumial Classification=SVM (Ahmadieh et al. 2023)	58.33	61.11	63.89	55.56	61.11	63.89	59.72	56.94	61.11	61.11	**60.28**	**61.11**
LSTM+ResNet+NN Classification=SVM (Ahmadieh et al. 2023)	59.72	61.11	63.89	56.94	61.11	65.27	61.11	59.72	62.50	62.50	**61.39**	**61.11**
LSTM+ResNet+ Fuzzy_Type1 Classification=SVM (Ahmadieh et al. 2023)	61.11	62.50	65.28	62.50	66.67	66.67	62.50	63.89	63.89	62.5	**63.75**	**65.28**
LSTM+ResNet+ Fuzzy_Type2 Classification=SVM (Ahmadieh et al. 2023)	65.27	63.89	66.67	65.28	68.06	69.44	63.89	65.28	66.67	66.67	**66.11**	**66.67**
LSTM+ResNet+ Nonlinear_Fuzzy_Type1 Classification=SVM	63.89	65.28	66.67	65.28	69.44	68.06	65.28	65.28	66.67	65.28	**66.11**	**66.67**
LSTM+ResNet+ Nonlinear_Fuzzy_Type2 Classification=SVM	66.67	66.67	68.06	66.67	72.22	70.83	66.67	66.67	68.06	68.06	**68.05**	**68.06**

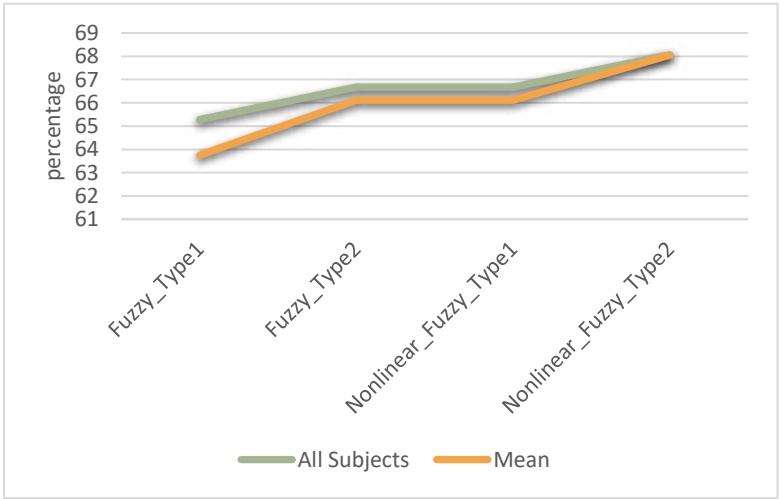

Fig. 13 Classification accuracy for comparing linear and nonlinear fuzzy systems for all participants (subject-independent), and mean of all participant

The results of the mean classification accuracy for all participants for the approaches implemented in this paper include LSTM with Softmax classification, polynomial, neural network, linear type-1 fuzzy, linear interval type-2 fuzzy (obtained in (Ahmadieh et al. 2023)), nonlinear type-1 fuzzy and nonlinear interval type-2 fuzzy (for this paper) are 55.55, 61.11, 61.11, 65.28, 66.67, 66.67 and 68.06 respectively. As can be seen in Table 4 and Fig. 14, the classification accuracy obtained for linear and nonlinear type-1 and type-2 fuzzy regression was higher than the best result obtained in (McCartney, Devereux, and Martinez-del-Rincon 2022; McCartney et al. 2019). The results of other methods implemented in this paper are very close to the results obtained in (McCartney, Devereux, and Martinez-del-Rincon 2022; McCartney et al. 2019). Also, the results of classification accuracy for the case that the regressions were trained with all participants for all the approaches implemented in this paper including LSTM with Softmax classification, polynomial, neural network, linear type-1 fuzzy, linear interval type-2 fuzzy, nonlinear type-1 fuzzy and nonlinear interval type-2 fuzzy are 55.83, 60.28, 61.39, 63.75, 66.11, 66.11 and 68.05 respectively. As shown in Table 4 and Fig. 14, in the case of nonlinear type-1 and interval type-2 fuzzy regression, obtained results are better than the best result reported in (McCartney, Devereux, and Martinez-del-Rincon 2022; McCartney et al. 2019) in the same condition. The results of other methods implemented in this paper are very close to the results the obtained in (McCartney, Devereux, and Martinez-del-Rincon 2022; McCartney et al. 2019).

The confusion matrix is a summary of the prediction results for a classification problem. The number of correct and incorrect predictions is summarized using counting values and divided by class. This is the key to the confusion matrix. Table 5 shows the classification accuracy for training and test data for all participants (subject-independent) and for one individual at random (third participant) according to the confusion matrix. Fig. 15 depicts Participant 3's Confusion Matrix for the 7 approaches outlined in Table 1 using test data.

Table 3 Classification precision, recall, and F1 score for all participants (subject-independent) for seven algorithms.

Method	Class	human body	human face	animal body	animal face	fruits/vegetables	tools
Method 1 **(Ahmadieh et al. 2023)**	**Precision**	58.33	50	41.66	72.72	54.54	57.14
	Recall	63.63	54.54	45.45	72.72	40	61.53
	F1score	60.86	52.17	43.47	72.72	46.15	59.25
Method 2 **(Ahmadieh et al. 2023)**	**Precision**	80	61.53	58.33	54.54	53.84	61.53
	Recall	66.66	66.66	58.33	50	58.33	66.66
	F1score	72.72	63.99	58.33	52.17	56.00	63.99
Method 3 **(Ahmadieh et al. 2023)**	**Precision**	75	71.42	63.63	54.54	58.33	66.66
	Recall	81.81	76.92	63.63	46.15	63.63	61.53
	F1score	78.26	74.07	63.63	50.00	60.86	63.99
Method 4 **(Ahmadieh et al. 2023)**	**Precision**	69.23	56.25	63.63	77.77	54.54	75
	Recall	81.81	69.23	58.33	53.84	54.54	75
	F1score	75.00	62.07	60.86	63.63	54.54	75.00
Method 5 **(Ahmadieh et al. 2023)**	**Precision**	75	75	58.33	58.33	66.66	66.66
	Recall	64.28	69.23	58.33	63.63	61.53	88.88
	F1score	69.23	72.00	58.33	60.86	63.99	76.18
Method 6	**Precision**	72.72	69.23	63.63	61.53	61.53	72.72
	Recall	66.66	75	58.33	66.66	66.66	66.66
	F1score	69.56	72.00	60.86	63.99	63.99	69.56
Method 7	**Precision**	75	66.66	58.33	63.63	75	75
	Recall	75	83.33	58.33	58.33	58.33	75
	F1score	75.00	74.07	58.33	60.86	65.62	75.00

Table 4 Classification accuracy of all participants (subject-independent) and mean of all participants for comparing the recommended methods in this paper with methods of the latest research with this dataset (McCartney et al. 2019).

EEG Features: **Image Feature:** **Feature Mapper:** **Classification:**	LSTM - - Softmax **(Ahmadieh et al. 2023)**	LSTM ResNet Polynomial SVM **(Ahmadieh et al. 2023)**	LSTM ResNet NN SVM **(Ahmadieh et al. 2023)**	LSTM ResNet Fuzzy_Type1 SVM **(Ahmadieh et al. 2023)**	LSTM ResNet Fuzzy_Type2 SVM **(Ahmadieh et al. 2023)**	LSTM ResNet NIT1FR SVM	LSTM ResNet NIT2FRS VM	Visual **(McCartney et al. 2019)**	Semantic **(McCartney et al. 2019)**	Visuo-semantic **(McCartney et al. 2019)**
All participants	55.55	61.11	61.11	65.28	66.67	66.67	68.06	61.97	64.82	66.01
Mean	55.83	60.28	61.39	63.75	66.11	66.11	68.05	58.08	60.88	62.02

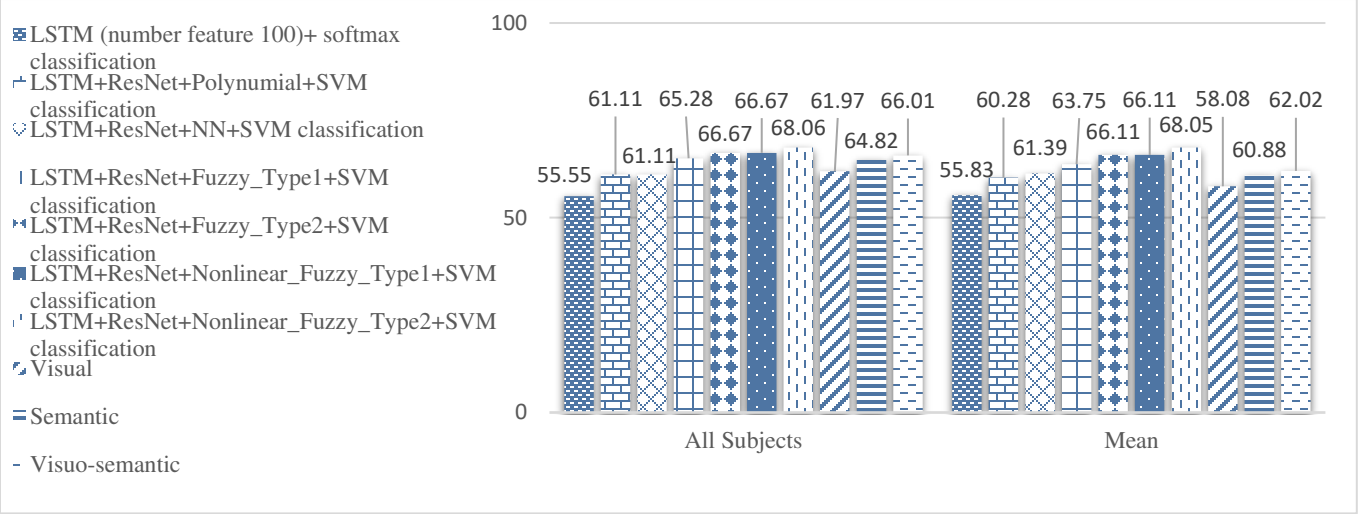

Fig. 14 Classification accuracy of all participants (subject-independent) and mean of all participants to compare with a classification accuracy of the three reported methods in (Ahmadieh et al. 2023; McCartney et al. 2019) with the same dataset.

Table 5 The classification accuracy for training and test data for all participants (subject-independent) and third participant (subject-dependent).

Participate	Classification accuracy Participate 3		Classification accuracy All Participate	
Method	Train	Test	Train	Test
LSTM (number feature 100) Classification=softmax (Ahmadieh et al. 2023)	83.43	58.33	80.65	55.55
LSTM+ResNet+Polynumial Classification=SVM (Ahmadieh et al. 2023)	82.72	63.89	79.94	61.11
LSTM+ResNet+NN Classification=SVM (Ahmadieh et al. 2023)	85.52	63.89	82.74	61.11
LSTM+ResNet+Fuzzy_Type1 Classification=SVM (Ahmadieh et al. 2023)	83.97	62.28	86.97	65.28
LSTM+ResNet+Fuzzy_Type2 Classification=SVM (Ahmadieh et al. 2023)	86.52	66.67	86.10	66.67
LSTM+ResNet+Nonlinear_Fuzzy_Type1 Classification=SVM	90.10	66.67	92.23	66.67
LSTM+ResNet+Nonlinear_Fuzzy_Type2 Classification=SVM	91.39	68.06	92.46	68.06

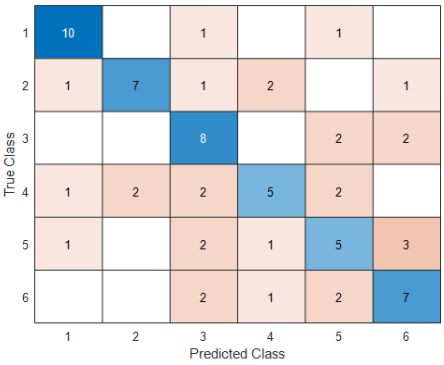

a) Accuracy=58.33

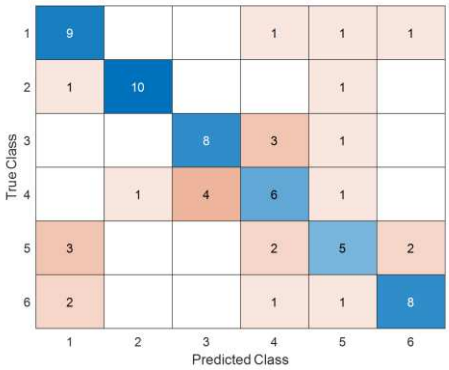

b) Accuracy=63.89

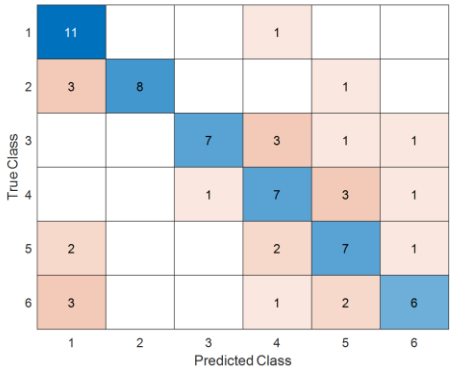

c) Accuracy=63.89

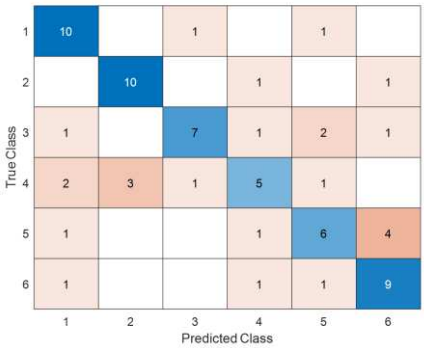

d) Accuracy=65.28

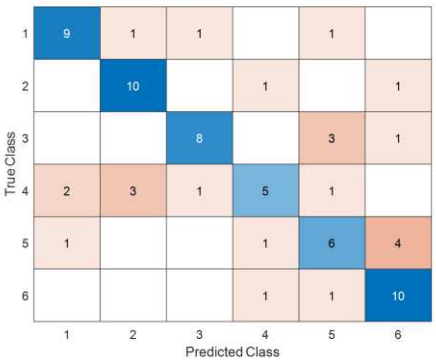

e) Accuracy=66.67

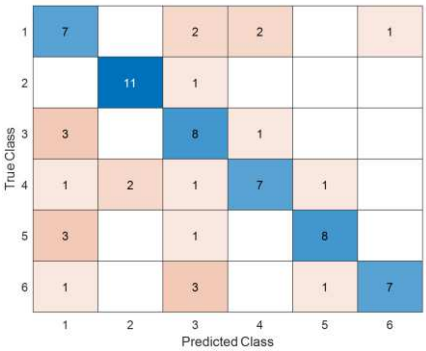

f) Accuracy=66.67

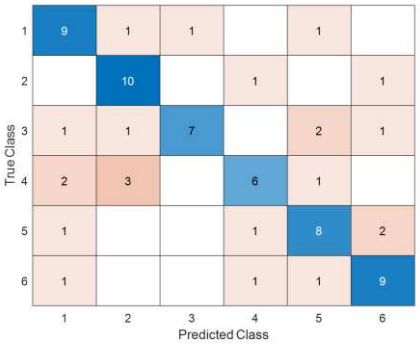

g) Accuracy=68.06

Fig. 15 Confusion matrix related to different test modes for participant 3. a) LSTM network and Softmax classifier b) Polynomial regression and classification with SVM c) Neural network regression and SVM classifier d) Type-1 fuzzy regression and classification with SVM e) Interval type-2 fuzzy regression and SVM classifier reported in (Ahmadieh et al. 2023) f) Nonlinear type-1 fuzzy regression and classification with SVM g) Nonlinear interval type-2 fuzzy regression and SVM classifier.

4. Discussion and Conclusion

This paper has presented a new method for the classification of visual images. In this regard, the LSTM network was used as a feature extractor from a two-dimensional EEG signal. Softmax was used for classification to ensure the quality of the features extracted from the LSTM network. Therefore, the average accuracy obtained with the bandpass filter used for preprocessing on all participants (subject-independent) in the Stanford dataset was 55.83%, which is a very good result compared to (Li et al. 2018, 2020) with the same conditions. In articles (Li et al. 2018, 2020; Spampinato et al. 2017), the accuracy of the classification is very low when the images are shown to people randomly and also the preprocessing is not done with the bandpass filter. The pre-trained ResNet network was then used to extract the features from the images. The network divided the 72 images into 6 groups by extracting 1000 features from each image. In the next step, the features extracted from the LSTM output and the features extracted from ResNet for each image are given to a linear and nonlinear interval type-2 and type-1 fuzzy, neural network, and polynomial regression as input. The difference between linear and nonlinear fuzzy regressions is in the function used in the consequent part of these networks, in the linear model the first-order polynomial function is used and in the nonlinear mode, the third-degree polynomial function is used. In the best case, the accuracy obtained after passing the EEG signal from the regression should be the same as the accuracy of the Resnet network classification for visual images. However, because EEG signals vary between participants and contain a significant level of noise, the classification accuracy in different modes for training data varies and is lower than the ResNet network classification accuracy (at best it is 98.61%). Finally, the SVM classifier was used to classify the images on the new features obtained for the new EEG signal.

The proposed method was implemented on a dataset provided by Stanford University. In 2019, this dataset was used for this purpose, in the best case, the classification accuracy was 62.2%, and here, the classification accuracy in the best case (when NIT2FR has been used) was 68.05%. Based on the findings, nonlinear fuzzy regression performed better than linear fuzzy methods, neural networks, and polynomial regression. This shows that fuzzy regression can perform better in conditions with high uncertainty. In addition, in both linear and nonlinear modes, due to the high uncertainty of the environment and the higher degree of freedom of type-2 fuzzy compared to type-1, type-2 fuzzy regression performed better than type-1 fuzzy regression. As we know, nonlinear systems in nonlinear environments can perform better than linear systems. In this paper, nonlinear fuzzy regression performed better than linear fuzzy regression.

In addition to accuracy, precision, recall, and F1 score are also used to evaluate the algorithms used in this paper. Nonlinear fuzzy type 2 regression, which had higher accuracy, had higher precision and recall in different classes on average, resulting in a higher F1 score. Also, these evaluators show a higher value in two non-linear type 1 and type 2 fuzzy algorithms than type 1 and 2 fuzzy.

By comparing the number of correct images in Fig. 15 in each class, it can be concluded that each of the regression methods used in this paper has strengths and weaknesses in different situations of EEG signals. We can use this to improve classification accuracy by combining the strengths of these regressions. In this paper, the gradient descent algorithm has been used to optimize regressions. As feature extraction plays an essential role in determining classification performance, future research would investigate alternative feature extraction methods instead of the LSTM networks. Finally, classifying images into groups serves as a foundation for more complex tasks, such as constructing images seen by participants using EEG signals.

Acknowledged:

This research did not receive any grant from funding agencies in the public, commercial, or non-profit sectors.

Conflict of Interest:

The authors have no conflicts of interest to declare that are relevant to the content of this article.

References

Acharya, U Rajendra, Shu Lih Oh, Yuki Hagiwara, Jen Hong Tan, Hojjat Adeli, and D Puthankattil Subha. 2018. 'Automated EEG-based screening of depression using deep convolutional neural network', *Computer methods and programs in biomedicine*, 161: 103-13.

Ahmadieh, Hajar, Farnaz Gassemi, Mohammad Hasan %J Neural Computing Moradi, and Applications. 2023. 'A hybrid deep learning framework for automated visual image classification using EEG signals': 1-17.

Alazrai, Rami, Motaz Abuhijleh, Mostafa Z Ali, and Mohammad I %J Expert Systems with Applications Daoud. 2022. 'A deep learning approach for decoding visually imagined digits

and letters using time–frequency–spatial representation of EEG signals', 203: 117417.

Brown, Emery N, Robert E Kass, and Partha P Mitra. 2004. 'Multiple neural spike train data analysis: state-of-the-art and future challenges', *Nature neuroscience*, 7: 456-61.

Byra, Michał, Grzegorz Styczynski, Cezary Szmigielski, Piotr Kalinowski, Łukasz Michałowski, Rafał Paluszkiewicz, Bogna Ziarkiewicz-Wróblewska, Krzysztof Zieniewicz, Piotr Sobieraj, and Andrzej Nowicki. 2018. 'Transfer learning with deep convolutional neural network for liver steatosis assessment in ultrasound images', *International journal of computer assisted radiology and surgery*, 13: 1895-903.

Coupland, Simon, and Robert John. 2008. 'Type-2 fuzzy logic and the modelling of uncertainty.' in, *Fuzzy sets and their extensions: Representation, aggregation and models* (Springer).

Craik, Alexander, Yongtian He, and Jose L. Contreras-Vidal. 2019. 'Deep learning for electroencephalogram (EEG) classification tasks: a review', *Journal of neural engineering*, 16: 031001.

Daliri, Mohammad Reza, Mitra Taghizadeh, and Kavous Salehzadeh Niksirat. 2013. 'EEG signature of object categorization from event-related potentials', *Journal of medical signals and sensors*, 3: 37.

Fang, Xing, and Zhuoning Yuan. 2019. 'Performance enhancing techniques for deep learning models in time series forecasting', *Engineering Applications of Artificial Intelligence*, 85: 533-42.

Fares, Ahmed, Shenghua Zhong, and Jianmin Jiang. 2018. "Region level bi-directional deep learning framework for eeg-based image classification." In *2018 IEEE International Conference on Bioinformatics and Biomedicine (BIBM)*, 368-73. IEEE.

Gadhoumi, Kais, Jean-Marc Lina, Florian Mormann, and Jean Gotman. 2016. 'Seizure prediction for therapeutic devices: A review', *Journal of neuroscience methods*, 260: 270-82.

Gers, Felix. 2001. 'Long short-term memory in recurrent neural networks', Verlag nicht ermittelbar.

He, Kaiming, Xiangyu Zhang, Shaoqing Ren, and Jian Sun. 2016. "Deep residual learning for image recognition." In *Proceedings of the IEEE conference on computer vision and pattern recognition*, 770-78.

Hisdal, Ellen. 1981. 'The IF THEN ELSE statement and interval-valued fuzzy sets of higher type', *International Journal of Man-Machine Studies*, 15: 385-455.

Hochreiter, Sepp, and Jürgen Schmidhuber. 1997. 'Long short-term memory', *Neural computation*, 9: 1735-80.

Jafakesh, Sara, Fatemeh Zareayan Jahromy, and Mohammad Reza Daliri. 2016. 'Decoding of object categories from brain signals using cross frequency coupling methods', *Biomedical Signal Processing and Control*, 27: 60-67.

Janssen, Ronald J, Janaina Mourão-Miranda, and Hugo G Schnack. 2018. 'Making individual prognoses in psychiatry using neuroimaging and machine learning', *Biological Psychiatry: Cognitive Neuroscience and Neuroimaging*, 3: 798-808.

Kamitani, Yukiyasu, and Frank Tong. 2005. 'Decoding the visual and subjective contents of the human brain', *Nature neuroscience*, 8: 679-85.

Kaneshiro, Blair, Marcos Perreau Guimaraes, Hyung-Suk Kim, Anthony M Norcia, and Patrick Suppes. 2015. 'A representational similarity analysis of the dynamics of object processing using single-trial EEG classification', *PloS one*, 10: e0135697.

Kappel, Simon L, David Looney, Danilo P Mandic, and Preben Kidmose. 2017. 'Physiological artifacts in scalp EEG and ear-EEG', *Biomedical engineering online*, 16: 1-16.

Khan, SanaUllah, Naveed Islam, Zahoor Jan, Ikram Ud Din, and Joel JP C Rodrigues. 2019. 'A novel deep learning based framework for the detection and classification of breast cancer using transfer learning', *Pattern Recognition Letters*, 125: 1-6.

Kingma, Diederik P, and Jimmy Ba. 2014. 'Adam: A method for stochastic optimization', *arXiv preprint arXiv:1412.6980*.

Krizhevsky, Alex, Ilya Sutskever, and Geoffrey E Hinton. 2012. "Imagenet classification with deep convolutional neural networks." In *Advances in neural information processing systems*, 1097-105.

Li, Ren, Jared S Johansen, Hamad Ahmed, Thomas V Ilyevsky, Ronnie B Wilbur, Hari M Bharadwaj, and Jeffrey Mark Siskind. 2018. 'Training on the test set? an analysis of spampinato et al.[31]', *arXiv preprint arXiv:1812.07697*.

Li, Ren, Jared S Johansen, Hamad Ahmed, Thomas V Ilyevsky, Ronnie B Wilbur, Hari M Bharadwaj, and Jeffrey Mark Siskind. 2020. 'The perils and pitfalls of block design for eeg classification experiments', *IEEE transactions on pattern analysis and machine intelligence*, 43: 316-33.

Malmivuo, Jaakko, Sari Ahokas, and Toni Välkky. 2014. "High-resolution EEG recording system using smart electrodes." In *2014 14th Biennial Baltic Electronic Conference (BEC)*, 21-24. IEEE.

McCartney, Ben, Barry Devereux, and Jesus %J Knowledge-Based Systems Martinez-del-Rincon. 2022. 'A zero-shot deep metric learning

approach to Brain–Computer Interfaces for image retrieval', 246: 108556.

McCartney, Ben, Jesus Martinez-del-Rincon, Barry Devereux, and Brian Murphy. 2019. 'Towards a real-world brain-computer interface for image retrieval', *bioRxiv*: 576983.

Miyawaki, Yoichi, Hajime Uchida, Okito Yamashita, Masa-aki Sato, Yusuke Morito, Hiroki C Tanabe, Norihiro Sadato, and Yukiyasu Kamitani. 2008. 'Visual image reconstruction from human brain activity using a combination of multiscale local image decoders', *Neuron*, 60: 915-29.

Münßinger, Jana I, Sebastian Halder, Sonja C Kleih, Adrian Furdea, Valerio Raco, Adi Hösle, and Andrea Kübler. 2010. 'Brain painting: first evaluation of a new brain–computer interface application with ALS-patients and healthy volunteers', *Frontiers in neuroscience*, 4: 182.

Murphy, Brian, Marco Baroni, and Massimo Poesio. 2009. "EEG responds to conceptual stimuli and corpus semantics." In *Proceedings of the 2009 Conference on Empirical Methods in Natural Language Processing*, 619-27.

Nguyen, Thanh, Abbas Khosravi, Douglas Creighton, and Saeid Nahavandi. 2015. 'EEG signal classification for BCI applications by wavelets and interval type-2 fuzzy logic systems', *Expert Systems with Applications*, 42: 4370-80.

Nijboer, Femke, EW Sellers, Jürgen Mellinger, Mary Ann Jordan, Tamara Matuz, Adrian Furdea, Sebastian Halder, Ursula Mochty, DJ Krusienski, and TM Vaughan. 2008. 'A P300-based brain–computer interface for people with amyotrophic lateral sclerosis', *Clinical neurophysiology*, 119: 1909-16.

Palazzo, Simone, Concetto Spampinato, Isaak Kavasidis, Daniela Giordano, and Mubarak Shah. 2017. "Generative adversarial networks conditioned by brain signals." In *Proceedings of the IEEE International Conference on Computer Vision*, 3410-18.

Park, Ho-Sung, Dong-Won Kim, and Sung-Kwun Oh. 2000. "Fuzzy Polynomial Neural Networks with Fuzzy Activation Node." In *Proceedings of the KIEE Conference*, 2946-48. The Korean Institute of Electrical Engineers.

Piccialli, Francesco, Vittorio Di Somma, Fabio Giampaolo, Salvatore Cuomo, and Giancarlo Fortino. 2021. 'A survey on deep learning in medicine: Why, how and when?', *Information Fusion*, 66: 111-37.

Shin, Hoo-Chang, Holger R Roth, Mingchen Gao, Le Lu, Ziyue Xu, Isabella Nogues, Jianhua Yao, Daniel Mollura, and Ronald M Summers. 2016. 'Deep convolutional neural networks for computer-aided detection: CNN architectures, dataset characteristics and transfer learning', *IEEE transactions on medical imaging*, 35: 1285-98.

Spampinato, Concetto, Simone Palazzo, Isaak Kavasidis, Daniela Giordano, Nasim Souly, and Mubarak Shah. 2017. "Deep learning human mind for automated visual classification." In *Proceedings of the IEEE conference on computer vision and pattern recognition*, 6809-17.

Tafreshi, Taban Fami, Mohammad Reza Daliri, and Mahrad Ghodousi. 2019. 'Functional and effective connectivity based features of EEG signals for object recognition', *Cognitive neurodynamics*, 13: 555-66.

Taghizadeh-Sarabi, Mitra, Mohammad Reza Daliri, and Kavous Salehzadeh Niksirat. 2015. 'Decoding objects of basic categories from electroencephalographic signals using wavelet transform and support vector machines', *Brain topography*, 28: 33-46.

Takagi, Tomohiro, and Michio Sugeno. 1985. 'Fuzzy identification of systems and its applications to modeling and control', *IEEE transactions on systems, man, and cybernetics*: 116-32.

Tirupattur, Praveen, Yogesh Singh Rawat, Concetto Spampinato, and Mubarak Shah. 2018. "Thoughtviz: visualizing human thoughts using generative adversarial network." In *Proceedings of the 26th ACM international conference on Multimedia*, 950-58.

Tonin, Luca, Tom Carlson, Robert Leeb, and José del R Millán. 2011. "Brain-controlled telepresence robot by motor-disabled people." In *2011 Annual International Conference of the IEEE Engineering in Medicine and Biology Society*, 4227-30. IEEE.

Wang, Fei, Mengqing Jiang, Chen Qian, Shuo Yang, Cheng Li, Honggang Zhang, Xiaogang Wang, and Xiaoou Tang. 2017. "Residual attention network for image classification." In *Proceedings of the IEEE conference on computer vision and pattern recognition*, 3156-64.

Wen, Haiguang, Junxing Shi, Wei Chen, and Zhongming Liu. 2018. 'Deep residual network predicts cortical representation and organization of visual features for rapid categorization', *Scientific reports*, 8: 1-17.

Wu, Dongrui. 2012. "Twelve considerations in choosing between Gaussian and trapezoidal membership functions in interval type-2 fuzzy logic controllers." In *2012 IEEE International conference on fuzzy systems*, 1-8. IEEE.

Yu, Renping, Lishan Qiao, Mingming Chen, Seong-Whan Lee, Xuan Fei, and Dinggang Shen. 2019. 'Weighted graph regularized sparse brain network construction for MCI identification', *Pattern Recognition*, 90: 220-31.

Zadeh, Lotfi A. 1965. 'Fuzzy sets', *Information and control*, 8: 338-53.

Zadeh, Lotfi A. 1975. 'The concept of a linguistic variable and its application to approximate reasoning-III', *information SCiences*, 9: 43-80.

Zheng, Xiao, Wanzhong Chen, Yang You, Yun Jiang, Mingyang Li, and Tao Zhang. 2020. 'Ensemble deep learning for automated visual classification using EEG signals', *Pattern Recognition*, 102: 107147.